CoA. Note M and P No.4.

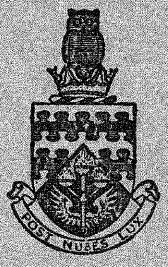

THE COLLEGE OF AERONAUTICS
CRANFIELD

CALCULATING THE SHEAR ANGLE IN ORTHOGONAL METAL CUTTING FROM FUNDAMENTAL STRESS-STRAIN-STRAIN RATE PROPERTIES OF THE WORK MATERIAL

by

P. L. B. Oxley and M. J. M. Welsh

CoA Note M. and P. No. 4.

March, 1964

THE COLLEGE OF AERONAUTICS

DEPARTMENT OF PRODUCTION AND INDUSTRIAL ADMINISTRATION

Calculating the shear angle in orthogonal metal cutting from fundamental stress-strain-strain rate properties of the work material*

- by -

P.L.B. Oxley and M.J.M. Welsh

SUMMARY

An analysis of the orthogonal metal cutting process is made which enables the shear angle to be calculated from certain fundamental properties of the work material and the specified cutting conditions. Shear angles are calculated for a range of cutting conditions and good agreement is shown between theory and experiment. In particular, such trends as the decrease in shear angle with decrease in cutting speed and the tendency for the chip to become discontinuous at slow cutting speeds which are found experimentally and cannot be explained in terms of previous shear angle analyses, are shown to be consistent with the present analysis.

---

* Given at the 4th International Machine Tool Design and Research Conference (1963) and reproduced by permission of Pergamon Press Ltd.

Introduction

In orthogonal metal cutting when cutting relatively ductile materials the magnitude of the shear angle (i.e. ϕ in Fig. 1) gives an indication of the efficiency of the process. Large values of shear angle are associated with cutting with a continuous chip (i.e. a chip formed by plastic deformation), resulting in a good surface finish and relatively low cutting force. With small values of shear angle the chip becomes discontinuous (i.e. fracture occurs), the surface finish deteriorates and the cutting force increases. Cutting conditions which tend to give a large value of shear angle are a high cutting speed, a large tool rake angle (i.e. α in Fig. 1) and a low frictional resistance along the tool chip surface.

There have been a number of attempts to predict the shear angle theoretically and, for example, Merchant[1] derived the shear angle equation.

$$\phi = \frac{\pi}{4} + \frac{\alpha}{2} - \frac{\lambda}{2} \qquad (1)$$

where λ is the mean angle of friction at the tool-chip interface. Another well known equation is that due to Lee and Shaffer[2], namely

$$\phi = \frac{\pi}{4} + \alpha - \lambda \qquad (2)$$

These equations show that a decrease in λ or an increase in α both lead to an increase in ϕ and this is consistent with experience. Unfortunately, when a wide range of cutting conditions is considered, both equations, and indeed all existing shear angle equations, show very poor quantitative agreement with experiment. It is apparent from experimental results that ϕ is dependent on cutting speed, depth of cut (t in Fig. 1) and work material properties. It is not surprising therefore, that existing shear angle equations, which are all independent of these parameters (except for associated variations in λ) show poor agreement with experiment.

In this paper an analysis is presented in which the cutting speed, depth of cut and certain fundamental work material properties are taken into account.

Theory

It is now generally accepted that the shear plane model of chip formation (Fig. 1), which assumes that the chip is formed by simple shear across a single shear plane, is inaccurate. Direct observations of chip formation have shown that the chip is formed in a finite plastic

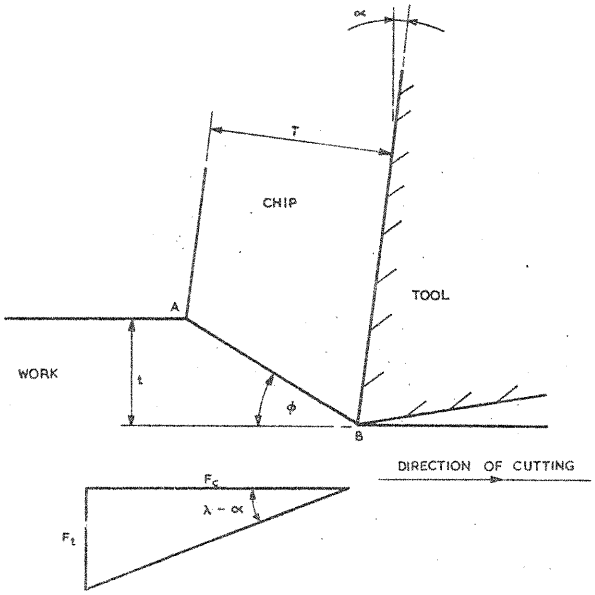

FIG. 1. Shear plane model of cutting.

01

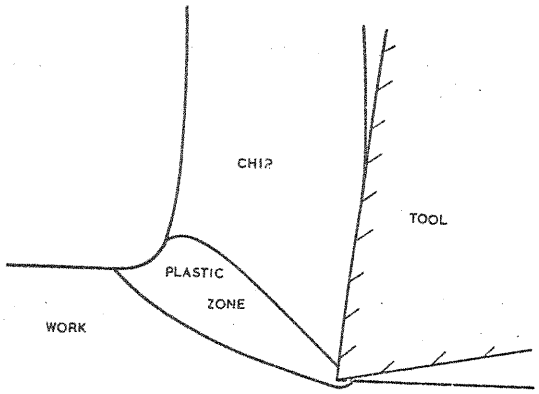

FIG. 2. Finite plastic zone.

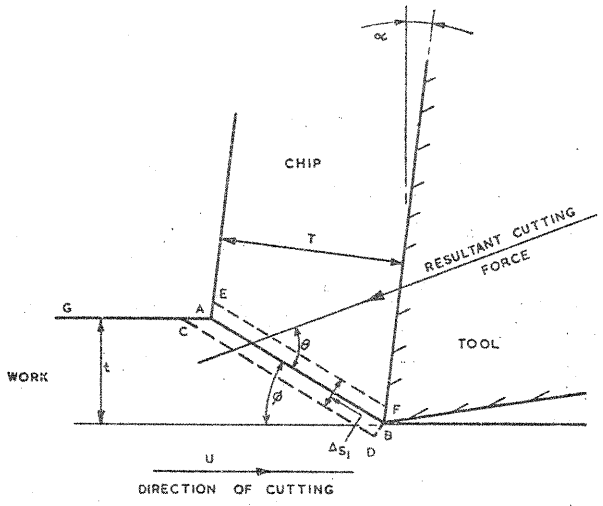

FIG. 3. Shear zone model of cutting.

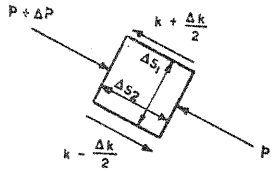

FIG. 4. Element of shear zone.

zone which is roughly of the shape shown in Fig. 2.

Following a recent analysis[3] let us idealize the finite plastic zone to the parallel-sided shear zone shown in Fig. 3 with CD, AB and EF straight parallel slip-lines representing the directions of maximum shear-stress and maximum shear-strain rate. Chip curl is, therefore, neglected and it is assumed that the state of strain, and therefore the shear flow stress, along each of the parallel slip-lines are constant. Let us further assume that we can represent the frictional condition along the tool-chip interface by a mean angle of friction λ.

Neglecting any up-thrust on the base of the tool, the slip-line AB (Fig. 3) will transmit the resultant cutting force and it is convenient to base our analysis on this slip-line. The method of analysis will be to analyse the stresses along AB and then to select the value of ϕ (i.e. the angle made by AB with the direction of cutting) to give a resultant cutting force direction across AB which is consistent with the direction given by considering the mean angle of friction at the tool-chip interface. From a geometrical viewpoint AB can be looked upon as the shear plane and ϕ as the shear angle, that is, from Fig. 3.

$$\tan \phi = \frac{t/T \cos \alpha}{1 - t/T \sin \alpha} \qquad (3)$$

where t is the depth of cut and T the chip thickness, and this equation is identical to that for the shear plane model of chip formation.

It was shown in a detailed analysis[4] of the stresses in the plastic zone that the hydrostatic stress in the region of A could be calculated most reliably from the free surface condition in the surface ahead of A. Let us therefore assume that AB bends to meet this free surface at 45 degrees (i.e. free surface condition) but does so in negligible distance. Then as p = k (compressive) at the free surface we can show from slip-line theory that

$$p_A = k \left[1 + 2 \left(\frac{\pi}{4} - \phi \right) \right] \qquad (4)$$

where p_A is the hydrostatic stress at A (i.e. the normal stress acting on AB at A) and k is the shear flow stress along AB.

Consider next the equilibrium of the small element of the shear zone shown in Fig. 4. As the material passes through the shear zone its shear flow stress will change, as a result of strain-hardening, temperature etc. Therefore, let the shear flow stress along CD (i.e. initial shear flow stress at zero plastic strain) be $k - \frac{\Delta k}{2}$, and let the

shear flow stress along EF be $k + \frac{\Delta k}{2}$. The total change in shear flow stress is then Δk. Resolving forces parallel to AB gives

$$\Delta p = \frac{\Delta k}{\Delta s_1} \cdot \Delta s_2$$

where Δp is the change in hydrostatic stress across the element, Δs_1 is the width of the shear zone and Δs_2 is measured along AB. Applying this equation between A and B (Fig. 3) we obtain

$$p_A - p_B = \frac{\Delta k}{\Delta s_1} \frac{t}{\sin \phi} \qquad (5)$$

or

$$p_B = p_A - \frac{\Delta k}{\Delta s_1} \frac{t}{\sin \phi}$$

where p_B is the hydrostatic stress at B (i.e. normal stress on AB at B). It is of interest to note that if Δk is positive, as we would in general expect it to be, then p_B has a smaller compressive value than p_A. Following the assumptions made, $\frac{\Delta k}{\Delta s_1}$ is constant along AB, and therefore the corresponding variation in hydrostatic stress along AB will be linear. It follows that if θ (Fig. 3) is the angle between the resultant cutting force and AB, then

$$\tan \theta = \frac{p_A + p_B}{2k} \qquad (6)$$

By considering the direction of the resultant cutting force determined by the mean angle of friction along the tool chip interface, it is easily shown that:

$$\theta = \phi + \lambda - \alpha \qquad (7)$$

Before equations (4), (5), (6) and (7) can be used to calculate ϕ it is necessary to know the value of Δk in equation (5). Let Fig. 5 represent the idealised shear flow stress-strain curve of the work material corresponding to the mean shear strain-rate in the shear zone (the slope of the curve and the initial yield stress will vary with strain-rate[5]). Then if the total shear strain occuring in the shear zone is γ we have

$$\Delta k = m.\gamma \qquad (8)$$

where m is the slope of the idealised stress-strain curve and where γ

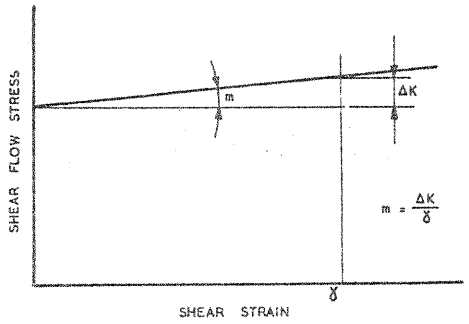

FIG. 5. Idealized shear flow stress–shear strain curve.

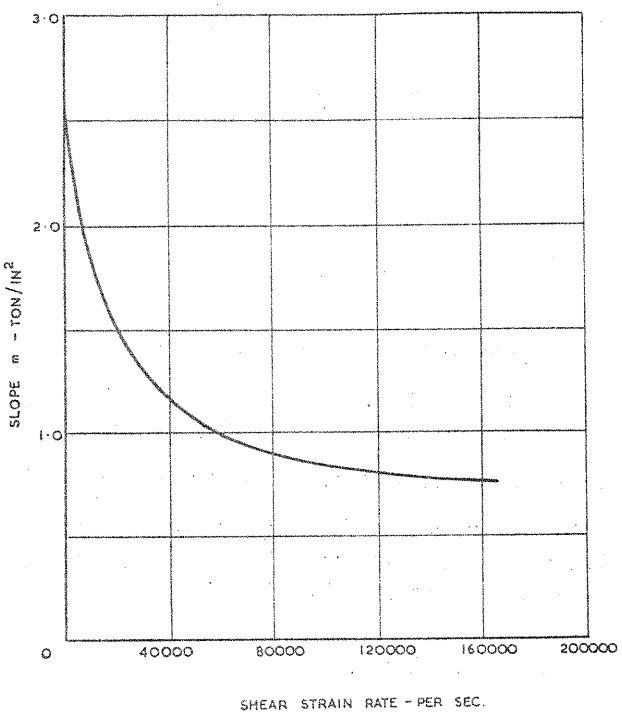

FIG. 6. Slope *m*.

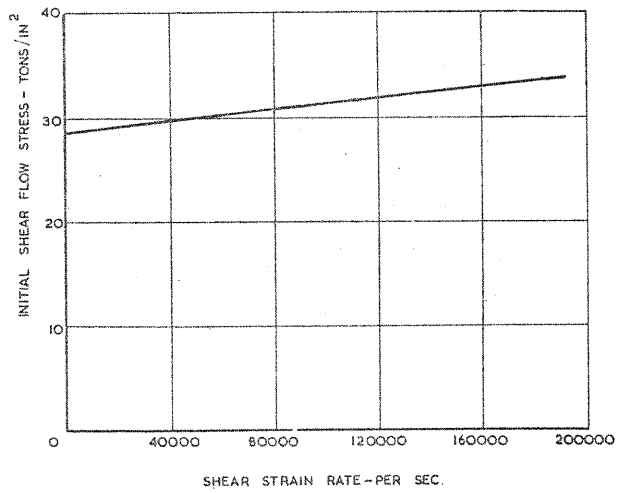

FIG. 7. Initial shear flow stress.

is given by (see ref. 5)

$$\gamma = \frac{\cos \alpha}{\sin \phi \cos (\phi - \alpha)} \tag{9}$$

In order to find m and also k (the shear flow stress along AB) we must know the mean shear strain-rate $\dot{\gamma}$ in the shear zone. In a recent analysis[5] this was shown to be given by the equation

$$\dot{\gamma} = \frac{0.2\, U \cos \alpha}{\Delta s_1 \cos (\phi - \alpha)} \quad \text{per sec.} \tag{10}$$

where U is the cutting speed in feet per minute and Δs_1 (the width of the shear zone) is in inches.

SHEAR ANGLE CALCULATIONS

Before the theory developed in the last section can be used to calculate values of shear angle, some assumption must be made as to the width of the shear zone (Δs_1 in Fig. 3). From the limited number of results available[6,7,8] it appears that the length to width ratio of the shear zone is reasonably constant. That is, although the width (Δs_1) changes with cutting conditions (for example, it increases with decrease in cutting speed) so does the length ($t/\sin \phi$) thus maintaining a shear zone of approximately constant proportions. For the purpose of our calculations let us assume that the ratio is constant, i.e.

$$\frac{t}{\Delta s_1 \sin \phi} = \text{const.} \tag{11}$$

From the measurements recorded the ratio is approximately equal to 10 and this is the value we shall take as our constant.

For the work material, we must know the values of the slope m (Fig. 5) and the initial shear flow stress for the range of shear strain-rate considered. These are apparently fundamental properties and indeed the variation of initial flow stress with strain-rate has been investigated directly. To the authors' knowledge no direct measurements of the slope m have been made.

Figs. 6 and 7 show graphs of the slope m and initial shear flow stress for a mild steel (SAE 1015, 118Bhn) obtained[5] by analysing cutting test results. Lacking any other information on the variations of m with strain-rate our calculations will be based on these graphs.

In making the calculations the most convenient method is to assume a particular value of ϕ, for given conditions of rake angle, depth of cut and cutting speed, and then to work through the equations to find the corresponding value of friction angle λ. Graphs of ϕ against $\lambda - \alpha$ can then be plotted in the usual way.

Let us now consider a specimen calculation, taking the following conditions:-

rake angle α = 30°
depth of cut t = 0.010 ins.
cutting speed U = 1,000 ft/min.

Assume ϕ = 30°
from equation (11) - (Const = 10)
Δs_1 = .002 in.

from equation (10)
γ = 86,600 per sec

referring to Figs 6 and 7
m = 0.87 ton/in^2

and the initial shear flow stress (k-Δk/2) = 31 ton/in^2

from equation (9)
γ = 1.73

from equation (8)
Δk = 1.5 ton/in^2

the shear flow stress, k, on CD (Fig. 3) is given by
k = initial shear flow stress (k - Δk/2) + Δk/2
= 31.75 ton/in^2

from equation (4)
p_A/k = 1.52

from equation (5)
$(p_A - p_B)/k$ = .47

hence p_B/k = 1.05

from equation (6)
θ = 52°

from equation (7)
$\lambda - \alpha$ = 22°

For α = 30° λ = 52°, we can now say that the analysis gives ϕ = 30°*

* There is a second possible solution which satisfies the equations, in which ϕ is much smaller, and this is true for the majority of cutting conditions (see for example Fig. 8 α = - 10° U = 1 ipm). The higher value of ϕ has been taken in each case as it gives the lower value of cutting force. The possibility of cutting with the second smaller value of shear angle should not be dismissed and will be considered in a future paper.

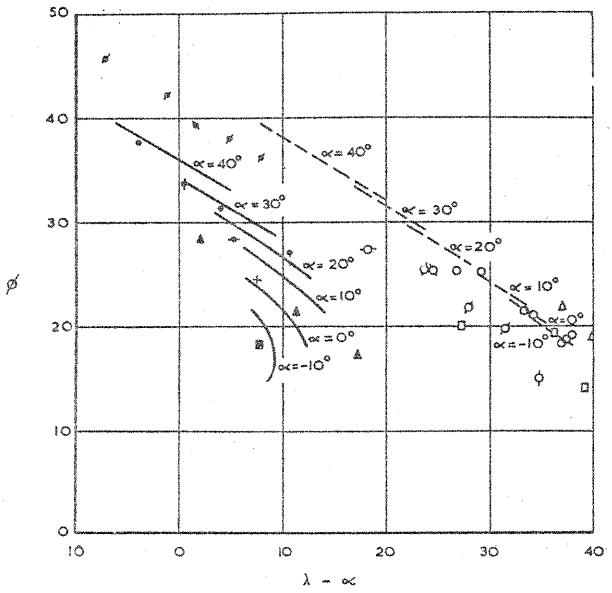

FIG. 8. Influence of cutting speed on shear angle.

Broken lines theoretical curves for 0·010 in. depth of cut, cutting speed 1000 ft/min, rake angles from −10° to 40°.
Unbroken lines theoretical curves for similar cutting conditions but 1 in./min cutting speed.
Experimental points:

Merchant[1]	a = 10°	○	400–1160 ft/min
	a = −10°	△	
Kececioglu[8]	a = −10°	□	
	a = 4°	○	
	a = 19·5°	⬠	746 ft/min
	a = 33°	⬠	
	a = 36·5°	⬡	
Shaw, Cook and Finnie[11]	a = 0°	▣	
	a = 16°	▲	
	a = 30°	◉	1 in./min
	a = 40°	◪	
Oxley[7]	a = 25°	+	
	a = 30°	⊕	0·5 in./min
	a = 35°	◍	
	a = 40°	◍	

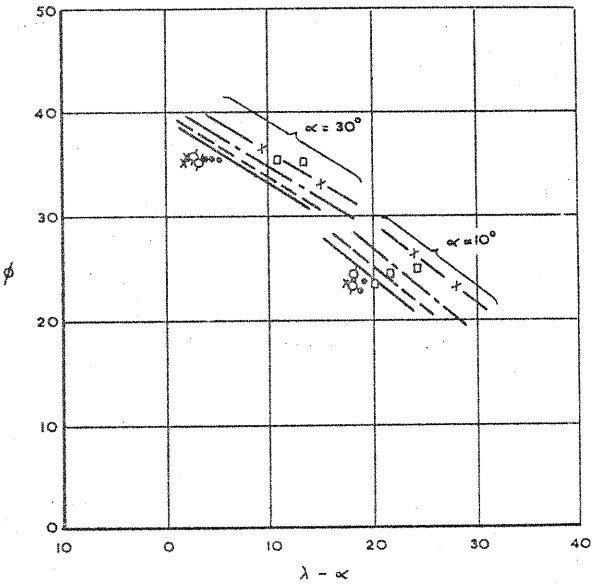

FIG. 9. Influence of depth of cut on shear angle.

Theoretical curves, cutting speed 100 ft/min
Rake angles 30° and 10°
Depth of cut 0·002 in. —— × —— × ——
0·004 in. — — — — — —
0·006 in. — — — — — —
0·008 in. ——————
Experimental points:

Kobayashi and Thomsen[9]	0·00198 in.	□
Cutting speed 90·8 ft/min	0·00401 in.	◉
Rake angles 30° and 10°	0·00631 in.	⬡
	0·00802 in.	×

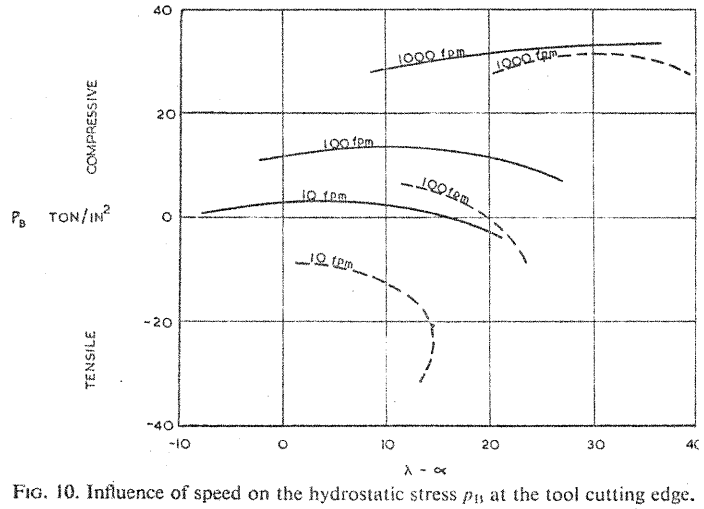

FIG. 10. Influence of speed on the hydrostatic stress p_B at the tool cutting edge.

Theoretical curves, cutting speed 10, 100 and 1000 ft/min, depth of cut 0·010 in.,
a = 30° ——————
a = 10° — — — — — —

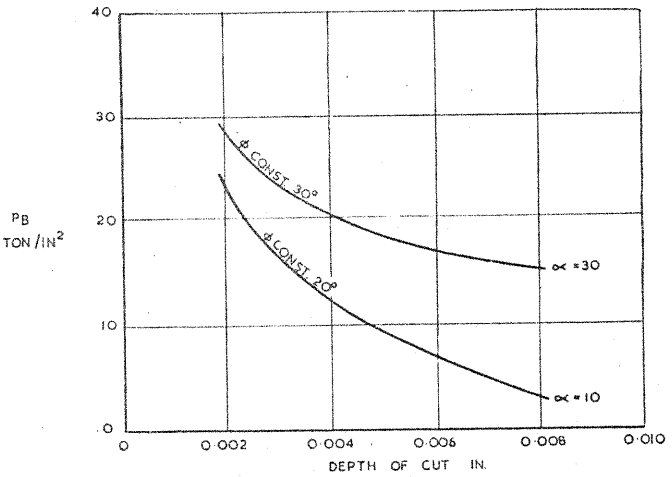

FIG. 11. Influence of depth of cut on the hydrostatic stress p_B at the tool cutting edge.

Using this method graphs of ϕ against $\lambda-\alpha$, for various rake angles, cutting speeds and depths of cut, have been obtained and are given in Figs. 8 and 9. The calculated values of the hydrostatic stress near the tool cutting edge (p_B) are given in Figs. 10 and 11.

DISCUSSION

Referring to Figs. 8 and 9 it can be seen that the theory predicts that for a given rake angle α and friction angle λ, a decrease in cutting speed or an increase in depth of cut t gives a decrease in shear angle ϕ. Experimental results show that, in general, these predictions are correct. A quantitative comparison between theoretical and experimental results is made difficult by the limited number of experimental results available, for the steel considered in the analysis. As this steel is apparently a typical mild steel, results obtained for other mild steels have also been used.[1,7,6,11].

The experimental values of ϕ and $\lambda-\alpha$ which are plotted in Figs. 8 and 9 were obtained from chip thickness ratio and cutting force measurements using equation (3) and the relation (see Fig. 1).

$$\tan(\lambda-\alpha) = Ft/Fc \qquad (12)$$

The agreement between the predicted and experimental values of ϕ is reasonably good, and, in particular, the influence of speed is clearly shown. Although the predicted increase in ϕ with decrease in depth of cut t is masked by an increase in λ (Fig. 9), the experimental results do follow the predicted trend. It is of interest that in considering the shear zone mechanism a decrease in t (depth of cut) has the same effect as an increase in the cutting speed i.e. both increase the shear strain-rate in the shear zone. The increase in shear strain-rate resulting from a decrease in t tends to increase the value of the shear flow stress, (Fig. 7) and this could account for the so-called size effect in metal cutting.

At present it is not possible to predict from a given state of stress, strain and strain-rate whether or not a material will fracture. It seems reasonable, however, to assume that the lower the compressive value of the hydrostatic stress near the tool cutting edge (p_B) the more likely is a chip to become discontinuous. If we accept this assumption it can be seen that according to the theory, the changes which would lead to a decrease in p_B and therefore tend to give a discontinuous chip are: a decrease in cutting speed, a decrease in rake angle and an increase in depth of cut. All of these changes are known in practice to be associated with the transition from a continuous to a discontinuous chip.

Although the curves of the slope n are not available for materials other than the one used in the analysis, there are cutting experiments

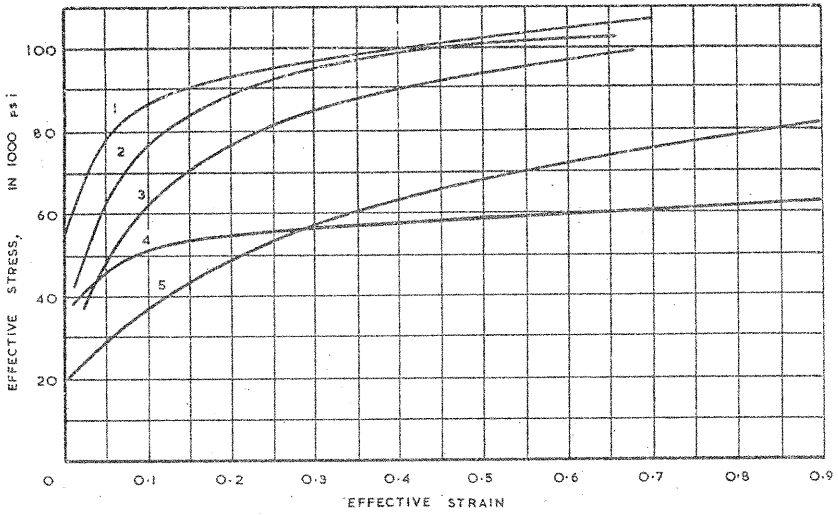

FIG. 12. Effective stress–strain curves (Kobayashi and Thomsen).[9]

1. SAE 1112 steel (as received)
2. 2024-T4 aluminium alloy
3. SAE 1112 steel (annealed)
4. 6061-T6 aluminium alloy
5. Alpha brass

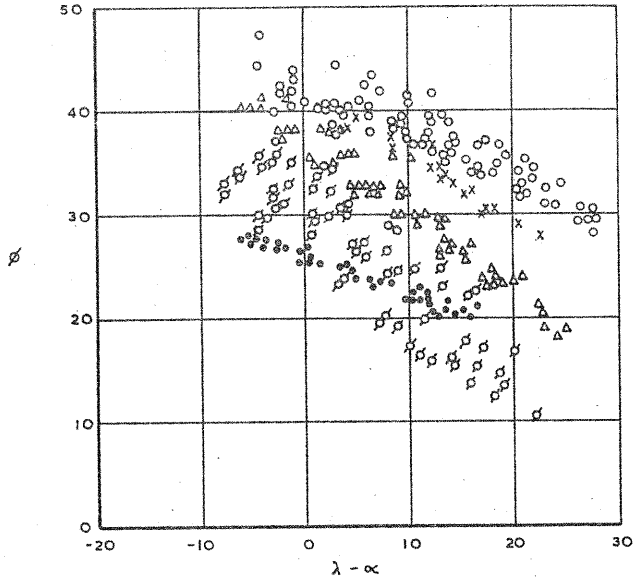

FIG. 13. Shear angle values for materials shown in Fig. 12 (Kobayashi and Thomsen).[9]

2024-T4 aluminium alloy ○
6061-T6 aluminium alloy ×
SAE 1112 steel (as received) △
SAE 1112 steel (annealed) ○
Alpha brass ●

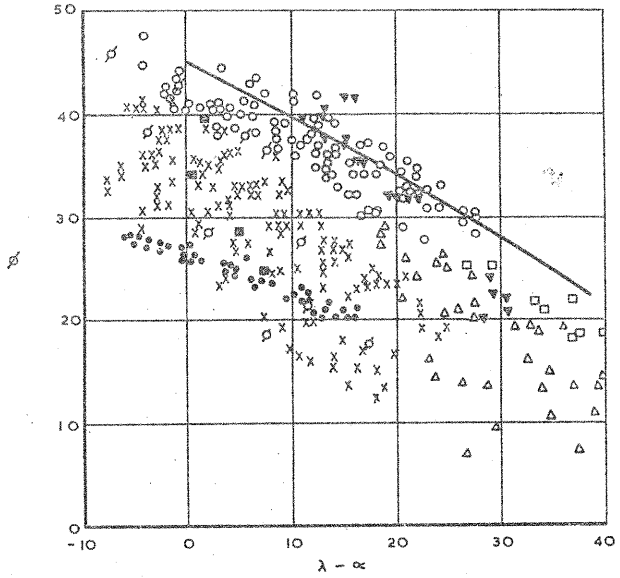

FIG. 14. Upper limit of shear angle solution.

Experimental points:
Merchant[1] □
Oxley[7] ■
Kececioglu[8] △
Kobayashi and Thomsen[9] Alpha brass ●
Aluminium ○
SAE 1112 ×
Shaw, Cook and Finnie[11] ◇
Thomsen, Lapsley and Grassi[12] ▼

reported[9] in which the effective stress-strain curves of the work material are given. If we assume that a high value of m from a static test is indicative of a comparably high value of m at higher strain rates then we can make some predictions as to the general order of shear angles for a particular material from its static stress-strain curve. From the calculations given in the previous section it can be seen that the significant parameter in calculating the change in hydrostatic stress across AB is not simply the slope m but the ratio m/k (where k is the shear flow stress along AB). Unfortunately k will depend on the shear strain along AB and cannot be determined until ϕ is known.

Consider the curves for the five materials shown in figure 12. For the purpose of estimating the relative range of shear angles for these materials let us take the value of k corresponding to an effective strain of 0.5; and since it has been shown[10] that it is the slope of the stress-strain curve at high strains rather than the initial slope which is important in metal cutting, let us take as our values of m the mean slope of the curves above an effective stress of 0.2.

[N.B. $\tau = \frac{\sigma_{eff}}{\sqrt{3}}$ and $\gamma = \sqrt{3}\,\epsilon_{eff}$ so that

$$\frac{m}{k} = \frac{\text{slope of effective stress-strain curve}}{\sqrt{3}\ \text{effective strain}}\ ]$$

TABLE 1

	Material	m/k
1.	SAE 1112 steel (as received)	.14
2.	2024 - T4 Aluminium alloy	.10
3.	SAE 1112 steel (annealed)	.25
4.	6061 - T6 Aluminium alloy	.11
5.	Alpha brass	.42

For given values of λ and α the theory predicts that the larger the value of m/k, the smaller will be the value of ϕ. Therefore from the values of m/k in Table 1, we can expect that the range of values of ϕ will be lowest for alpha brass and then in the order, SAE 1112 annealed, SAE 1112 as received, 6061 - T6 Al, 2024 - T4 A. Experimental values of ϕ for these materials (Fig. 13) confirm this trend.

Let us assume that the limiting value of m as strain-rate increases is zero (i.e. non-strain-hardening material). By applying the analysis we obtain the line shown in Figure 14 (which is independent of α). This line can now be looked upon as setting an upper limit to values of ϕ, above which an increase in strain-rate (brought about by an increase in cutting speed or a decrease in depth of cut) will have no effect. Experimental values for a wide range of cutting conditions and work materials are plotted in Figure 14 and it can be seen that most of these results fall below the limiting line. A possible reason for points which fall above this line is that strain-softening (i.e. negative m) occurred during cutting. A more likely explanation, however, is to be

found in the simplifying assumptions which have been made in the analysis. Let us now consider these assumptions and their limitations in some detail.

It would be very surprising if the shear zone length to width ratio ($t/\Delta s_1 \sin \phi$) remained constant (assumed equal to 10 in the calculations) for all materials and cutting conditions. From the few measurements which have been made (limited to mild steel) it appears that the ratio decreases slightly with reduction in cutting speed.[7,8] Allowing for this reduction would emphasise the difference between the results for slow and high speed cutting, predicted in the analysis. The actual shape of the shear zone is also important and although we have assumed a parallel-aided zone it is now generally accepted that the width of the zone decreases towards the cutting edge of the tool. With such a zone the hydrostatic stress distribution along AB would not be linear and equations (5) and (6) would be modified. Photographic investigations of the shear zone are now being made in order to determine the size and shape of the zone for a wide range of cutting conditions and work materials.

In the analysis a mean value of shear strain-rate has been defined and used to find the corresponding mean value of the slope m. It is known from experiments[7] that the shear strain-rate and therefore m vary from point to point in the shear zone; for many materials m is also a function of the shear strain. As a result of the variation of shear strain in the shear zone the chip is 'born' curled and does not flow parallel to the tool over its full thickness as assumed in the analysis. A more detailed analysis will have to take into account these variations in shear strain-rate and shear strain, and also chip curl.

In the analysis no attempt has been made to show that the values of the hydrostatic stress at B(p_B) calculated from equation (5), are consistent with the frictional conditions at the tool cutting edge. (In an earlier paper[3] this boundary condition was used to find p_B directly.) There are two main reasons for this, first it is very difficult to say from a measurement of the mean angle of friction at the tool-chip interface just what the frictional conditions at the cutting edge are, and second the stress gradients in the shear zone adjacent to the cutting edge can be very large. In the photographic investigations mentioned above, particular attention is being paid to the flow round the cutting edge. The influence of a built-up edge (neglected in the analysis) is also being investigated.

It can be concluded that, in spite of the limitations imposed by the various simplifying assumptions made, the analysis gives at least a qualitative explanation of the main trends observed in cutting. Further work both theoretical and experimental, should lead to a more precise analysis.

Acknowledgements

The authors would like to thank Professor J. Loxham, Head of the Department of Production and Industrial Administration, College of Aeronautics, Cranfield for his interest and help, and also the Production Tool Alloy Co. for making possible the participation of one of the authors in the investigation.

REFERENCES

1. M.E. Merchant, J. Appl. Phys. 16, 267 and 318 (1945)

2. F.H. Lee and B.W. Shaffer, J. Appl. Mech. 18, 405 (1951)

3. P.L.B. Oxley, A.S.M.E. Paper No. 62 - WA - 74 (1963)

4. W.B. Palmer and P.L.B. Oxley, Proc. I. Mech. E. 173,24,623 (1959)

5. P.L.B Oxley, A.S.M.E. Paper No. 62 - WA - 139 (1963)

6. K. Nakayama, J. Soc. Pron. Mech. Japan 23, 491 (1957)

7. P.L.B. Oxley, Leeds University, Ph.D. Thesis (1957)

8. D. Kececioglu, Trans. A.S.M.E., 80, 158 (1958)

9. S. Kobayashi and E.G. Thomsen, Trans. A.S.M.E., Series B, J. Eng. for Ind. 81, 251, (1959)

10. P.L.B. Oxley, A.G. Humphreys and A. Larizadeh, Proc. I. Mech. E. 175, 18, 881 (1961)

11. M.C. Shaw, N.H. Cook and I. Finnie, Trans. A.S.M.E. 75,273 (1953)

12. E.G. Thomsen, J.T. Lapsley and R.C. Grassi, Trans. A.S.M.E. 75, 591 (1953).